

How to cite: *Angew. Chem. Int. Ed.* **2023**, 62, e202302483
doi.org/10.1002/anie.202302483

Photocatalysis

Photocatalytic Metal Hydride Hydrogen Atom Transfer Mediated Allene Functionalization by Cobalt and Titanium Dual Catalysis

Huaipu Yan⁺, Qian Liao⁺, Yuqing Chen, Gagik G. Gurzadyan, Binghui Lu, Chao Wu, and Lei Shi*

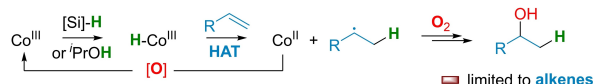
Abstract: Catalytic metal hydride hydrogen atom transfer (MHAT) reactions have proven to be a powerful method for alkene functionalization. This work reports the discovery of Co-porphines as highly efficient MHAT catalysts with a loading of only 0.01 mol % for unprecedented chemoselective allene functionalization under photoirradiation. Moreover, the newly developed bimetallic strategy by the combination of photo Co-MHAT and Ti catalysis enabled the successful carbonyl allylation with a wide range of amino, oxy, thio, aryl, and alkyl-allenes providing expedient access to valuable β -functionalized homoallylic alcohols in over 100 examples with exceptional regio- and diastereoselectivity. Mechanism studies and DFT calculations supported that selectively transferring hydrogen atoms from cobalt hydride to allenes and generating allyl radicals is the key step in the catalytic cycle.

studied and have led to practical methods for forming C–C and C–heteroatom bonds (Figure 1a).^[7–15] The outstanding functional group tolerance, excellent chemoselectivity, and ease of execution, made them enabling tools for nature products synthesis and late-stage reactions of complex molecules.^[16–23] However, despite significant achievements have been made for alkene functionalization, MHAT-mediated chemoselective functionalization of allenes remains undeveloped, because an efficient catalytic MHAT system that can distinguish between allenes and resulting alkenes has not been established (Figure 1c).^[24]

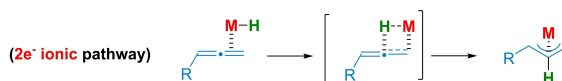
Introduction

The development of more efficient and sustainable synthetic strategies is the key driving force behind the continuous advancement of organic synthesis.^[1,2] Molecule-assisted homolysis, which occurs when two non-radical species interact to form radicals, is a fundamental chemical reaction.^[3–6] Catalytic MHAT reactions with alkenes, pioneered by Halpern and Mukaiyama, have been extensively

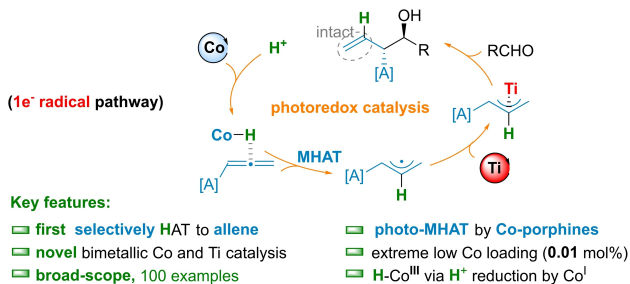
a) Classical **alkene** functionalization by **MHAT**, represented by Mukaiyama hydration



b) Well established: migratory insertion of **allene** into **metal-hydride**



c) Conceptually novel merging **photocatalytic Co-MHAT** and π -allylmetals chemistry



d) aminoalcohol, diol, and thioalcohol in drug and natural product

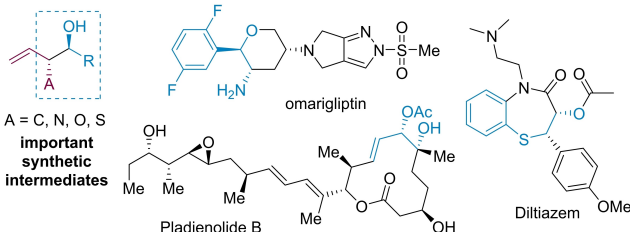


Figure 1. a) Mukaiyama hydration; b) Migratory insertion of allene into metal-hydride; c) Conceptually novel allene functionalization by photoredox Co-MHAT and Ti dual catalysis; d) Representative drugs/natural products containing 1,2-aminoalcohol, 1,2-diol, and 1,2-thioalcohol.

[*] H. Yan,⁺ Q. Liao,⁺ Y. Chen, L. Shi
State Key Laboratory of Fine Chemicals, School of Chemistry,
Dalian University of Technology
Dalian, 116024 (China)
E-mail: shilei17@dlut.edu.cn

G. G. Gurzadyan
State Key Laboratory of Fine Chemicals, Institute of Artificial
Photosynthesis, Dalian University of Technology
Dalian, 116024 (China)

B. Lu, L. Shi
School of Chemistry and Chemical Engineering, Henan Normal
University
Xinxiang, 2453007 (China)

C. Wu
Frontier Institute of Science and Technology, Xi'an Jiaotong
University
Xi An Shi, Xi'an, 710054 (China)

[†] These authors contributed equally to this work.

The addition of π -allylmetal complexes to carbonyls is one of the most important and reliable C–C bond-forming reactions for synthesizing homoallylic alcohols.^[25–29] Particularly, vinyl-substituted 1,2-aminoalcohols, 1,2-diols, and 1,2-thioalcohols are versatile synthetic intermediates frequently used in the synthesis of bioactive natural products and drugs, tethering an alkene group facilitates downstream synthetic manipulations (Figure 1d).^[30–33] Unfortunately, synthesizing of nucleophilic 3-[A]-allylic-metal reagents that bear a hetero-atom (A = N, O, S) from corresponding allylic halides precursors (e.g. 3-alkoxyallyl-metal) is laborious and inconvenient.^[34] An alternative method involves the use of readily available amino, oxy, thio, aryl, and alkyl-allenes as promising alternative allyl sources for transition metal-catalyzed carbonyl allylation. Although less developed, Krische and co-workers recently elegantly demonstrated Ir- and Ru-catalyzed amino-allenes allylation.^[35–37]

In contrast to the traditional ionic ($2e^-$) pathway (e.g. migratory insertion of allene to metal hydride, Figure 1b),^[38,39] radical ($1e^-$) generation of π -allylmetal complexes from dienes and alkenes has provided an alternative strategy to unlock unconventional transformations.^[40] Interestingly, the generation of π -allylmetal complexes from allenes triggered by H atom transfer has not been explored.^[41–45] Inspired by the recent advancements in photoredox/Co catalysis,^[46–49] and the pioneered work in photoredox/Ti chemistry by Gansäuer and other groups,^[50,51] we propose using H-Co^{III}, which is generated through the reduction of H⁺ by Co^I^[17,22,52] for MHAT reactions to selectively transfer H atom to allene ($1e^-$ pathway). This would result in the formation of a transient allyl radical which could be quickly intercepted by Ti^{III} to produce nucleophilic π -allyltitanium complexes for aldehyde allylation. Our approach would significantly increase the synthetic value of classical MHAT reactions and broaden the scope for carbonyl allylation (Figure 1c).

To achieve this strategy, several challenges need to be overcome. These include 1) how to enable H atom transfer to allene rather than the migratory insertion of allene to H-Co, 2) can Co–H distinguish between allenes and alkenes in allylic products, 3) how to avoid the direct reduction of carbonyls by Co–H species,^[53] 4) diastereoselectivity may be affected by the presence of heteroatoms.^[54]

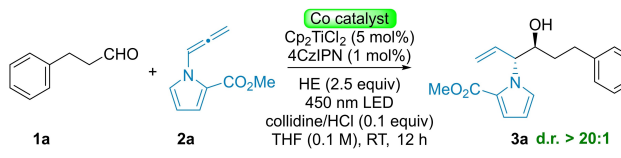
Herein, by the successful merging MHAT and π -allylmetal chemistry, we present a conceptually new synthesis of π -allylmetal complexes from allenes via a sequential H atom and $1e^-$ transfer approach for carbonyl allylation. The novel and simple bimetallic Co/Ti photoredox catalysis shows broad compatibility with various amino, oxy, thio, aryl, and alkyl-allenes and provides rapid access to the valuable β -functionalized homoallylic alcohols with exceptional regio- and diastereoselective control.

Results and Discussion

The study began by using standard substrates phenylpropyl aldehyde **1a** and pyrrole-derived aminoallene **2a** in the presence of titanocene dichloride (Cp₂TiCl₂), 2,4,5,6-tetra-

9H-carbazol-9-yl-1,3-benzenedicarbonitrile (4CzIPN), and Hantzsch ester (HE) in tetrahydrofuran (THF) with 450-nm LED irradiation. Multiple Co-complexes reported to generate H–Co species were tested but failed to catalyze the reaction (Table 1, entry 1).^[17–21] Excitingly, when Co-phthalocyanine **Co-4** was used desired 1,2-aminoalcohol derivative **3a** was obtained in a decent yield of 48 % (entry 2). After examining structurally similar Co-porphines (Por),^[55] Co-(Por)-OMe **Co-1** was found to have much better reactivity, yielding 83 % of **3a** with only 1 mol % loading and an impressive 93 % yield with 0.1 mol % loading (entry 3 and 4). Fine-tuning the electronic properties of Co-porphines had significant effects on catalytic activity. Co(Por)-CN **Co-3** showed the highest reactivity, affording **3a** in excellent 95 % yield with loading as low as 0.01 mol % (entries 5–7). Remarkably, the novel Co/Ti dual catalysis exhibited outstanding diastereoselectivity control (d.r. > 20:1). The catalytic amount of collidine/HCl was enough to enable the

Table 1: Reaction Optimization.^[a,b]



Reaction scheme: **1a** + **2a** $\xrightarrow[\text{collidine/HCl (0.1 equiv), THF (0.1 M), RT, 12 h}]{\text{Co catalyst, Cp}_2\text{TiCl}_2 \text{ (5 mol\%)}, \text{4CzIPN (1 mol\%)}, \text{HE (2.5 equiv)}, \text{450 nm LED}}$ **3a** (d.r. > 20:1)

Chemical structures of Co catalysts:

- Co-1**: R = OMe, CoPor-OMe
- Co-2**: R = H, CoPor-H
- Co-3**: R = CN, CoPor-CN
- Co-4**: CoPC
- Co-5**: CoBr₂ + dppp
- Co-6**: CoBr₂ + Xantphos
- Co-7**: CoBr₂ + DPEPhos
- Co-8**: CoBr₂ + dtbbpy
- Co-9**: Co(dmgH)₂PyCl(II)
- Co-10**: Co(salen)
- Co-11**: Co(acac)₃

Entry	Variation from standard conditions	Yield [%]
1	Various Co catalysts (Co-5,6,7,8,9,10,11)	0
2	CoPC Co-4 (1 mol %)	48
3	CoPor-OMe Co-1 (1 mol %)	83
4	CoPor-OMe Co-1 (0.1 mol %)	93 (91) ^[c]
5	CoPor-OMe Co-1 (0.01 mol %) 24 h	60
6	CoPor-H Co-2 (0.01 mol %) 24 h	33
7	CoPor-CN Co-3 (0.01 mol %) 24 h	95
8–13	in entries 8–13, Co-1 (0.1 mol %) was used	
8	No collidine/HCl	< 10
9	TMSCl (2 equiv) instead of collidine/HCl	50
10	Et ₃ N or DIPEA instead of HE	0
11	Zn (3 equiv) and collidine/HCl (2 equiv) instead of 4CzIPN and HE	0
12	No Cp ₂ TiCl ₂ /Co/4CzIPN/HE/hv	0
13	CrCl ₃ , CoBr ₂ , NiCl ₂ , FeCl ₃ , and Cu(OAc) ₂ instead of Cp ₂ TiCl ₂	0

[a] Reaction conditions: **1a** (0.2 mmol), **2a** (0.4 mmol). [b] Yields were determined by ¹H NMR spectroscopy versus an internal standard (1,3,5-trimethoxybenzene). [c] Isolated yield. TMSCl: chlorotrimethylsilane; Et₃N: triethylamine; DIPEA: N,N-diisopropylethylamine.

reaction to proceed, as the yield of **3a** dropped greatly to less than 10 % without it (entry 8). Although additives like TMSCl enabled the reaction to proceed, the yield was only moderate at 50 % (entry 9). Other organic electron donors, such as Et₃N and DIPEA, did not result in any product (entry 10), nor did Zn dust as a terminal reductant (entry 11). The reaction did not proceed in the absence of Cp₂TiCl₂, CoPor, 4CzIPN, HE, or visible light (entry 12). Notably, none of the other metals tested, including Cr, Co, Ni, Fe, and Cu, catalyzed the reaction under the same conditions (entry 13). The reaction was sensitive to high oxygen concentration, as revealed by condition-based sensitivity screening (for details please see Supporting Information S5).^[56]

Under the optimized reaction conditions, the Co/Ti dual catalysis system proved to be effective in enabling the allylation of the diverse substrates, including aliphatic and aromatic aldehydes, and amino allenes. The reaction furnished a library of structurally varied vinyl-substituted 1,2-aminoalcohol derivatives with high yields and excellent diastereoselectivity. (Table 2). The process was conducted under mild photo conditions ensuring excellent compatibility with important and sensitive functional groups, such as alkyne **3e**, alkene **3o**, free phenol **3c** and **4e**, alcohol **4c**, alkyl halide **3j**, and ether **4g**. The electronics and position of substituents on the aromatic rings affected diastereoselectivity and reaction efficiency (**4a–4g**). Incorporation of electron-rich *p*-anisaldehyde produced **4b** in high yield (80 %; d.r. = 15:1), while electron-poor *p*-fluorobenzaldehyde furnished **4f** in lower yield (55 %; d.r. > 20:1).

Additionally, Allylation of conjugated 3,3-dimethylacrolein **3k**, sterically hindered mesitaldehyde **4d**, and cyclopropanecarboxaldehyde **3l** occurred successfully. Heteroatoms, such as oxygen and nitrogen, in **3f**, **3h**, **3g**, and **3i**, and heteroarenes, including furan **4i**, thiophene **4j**, and indole **4h** were all compatible with the Co/Ti dual catalysis system. Investigation of amino-allenes revealed that N-phthalimide **5k**, unsubstituted pyrrole **5l**, and electron-poor pyrrol-2-carbonitrile **5h** were suitable substrates, yielding the corresponding alcohols in nice yields. N-phthalimide **5k** and unsubstituted pyrrole **5l** were easily removed under mild conditions to produce free 1,2-aminoalcohol **5m** in decent yields of 72 % and 50 % respectively. Indoles and their derivatives are highly desirable moieties in pharmaceutical applications and are frequently found in natural products. Transformation of indole-based allenes, including 2-phenylindole **5c**, 4-bromoindole **5d**, 3-cyanoindole **5e**, 3-carboxylate indole **5f**, and 7-azaindole **5g**, resulted in N-allylic indoles with excellent diastereoselectivity control (d.r. > 20:1).

Homoallylic 1,2-diols and thioalcohols play a crucial role in the synthesis of carbohydrates and drugs. However, their diastereoselective synthesis through catalysis remains challenging owing to the strong coordination of oxygen/sulfur atoms to metals.^[54] Excitingly, the modularity of the Co/Ti dual catalysis enabled the efficient synthesis of numerous homoallylic 1,2-diols/thioalcohols with nice anti-diastereoselectivity from oxy/thio-allenes as illustrated in table 3. Various substituted aryloxy-allenes could accommodate

allylation reactions in generally decent yields and diastereoselectivity. With the use of strong electron-withdrawing groups like *p*-CF₃ **8c** and *p*-CN **8d**, moderate diastereoselectivity (d.r. = 5:1) was observed. Notably, the reaction can be applied to both primary and secondary aldehydes containing heteroatoms (**8e–8q**, **9a–9n**). Interestingly, allylation of 2-benzoxazolylthiol-allene with various aldehydes afforded linear homoallylic alcohols in good *E* selectivity (**9o–9t**). This strategy provides a simple and efficient approach to the production of alkenyl sulfide.

Furthermore, the dual catalysis can efficiently catalyze allylation with various carbon-allenes to produce homoallylic alcohols (Table 4).^[57–59] To our surprise, the alkylallenes, which were challenging substrates in the previous work, gave the products with excellent diastereoselectivity (**11h–11l**). Surprisingly, disubstituted allenes, such as α -methylphenylallene, also proved to be good substrates in the catalysis strategy, producing homoallylic alcohols featuring quaternary carbon centers with excellent regio- and diastereoselectivity control (**11m–11p**).

The scalability of the catalytic system was determined through gram-scale synthesis of **3n**, **5e**, and **9a**, which yielded satisfying results (75 %, 87 %, and 75 %, respectively) as shown in Figure 2b. Additionally, the viability of the Co/Ti dual catalysis system was demonstrated through the late-stage functionalization of complex molecular structures, including the successful synthesis of **12c** in good yield from the estrone derivative (Figure 2a) without the addition of ketone. To explore the synthetic applications of homoallylic 1,2-aminoalcohol derivatives, **5e** was subjected to PPh₃ and DEAD, resulting in the elimination of the secondary alcohol to afford 2-amine diene **15**. The efficient conversion of **5m** to vinyl-oxazolidinone **13a** and vinylaziridine **13b**, both of which are prevalent in natural products, was also demonstrated (Figure 2c).

In Figure 3, the reaction profile was analyzed, but no obvious incubation period was observed. The consumption of **1a** and **2a** was similar and steady generation of **3a** was observed, completing the reaction within eight hours.

Further mechanistic experiments were performed to identify the radical nature of the reaction and elucidate the role of Co-porphine catalyst. 2,2,6,6-Tetramethylpiperidinoxyl (TEMPO) completely inhibited the reaction under standard conditions (Figure 4a). When **2a** reacted without Cp₂TiCl₂ and aldehydes, the allyl radical adduct **17** was obtained in 22 % yield (Figure 4b), ambiguously demonstrating the existence of allyl radical **16**. When **Co-6** or **Co-7** were used instead of **Co-1**, **2a** was fully consumed but adduct **17** was not obtained, possibly indicating that H-**Co-6** and H-**Co-7** underwent migratory insertion with allene as H-**Co-1** underwent H atom transfer pathway. When Co catalyst was absent, **2a** was recovered (Figure 4c), demonstrating that Co-1 was necessary for the generation of allyl radical **16** but not associated with Cp₂TiCl₂.

Deuterium experiments were conducted with *d*₁-HE, *d*₂-HE, and *d*₃-HE (Figure 4d), with a deuterium found in the 2-position of the allene in all cases. The product contained no deuterons when *d*₈-THF was used as the solvent. These results align with the proposed H-Co MHAT mechanism.

Table 2: Scope of allylation with amino-allenes.

$\text{RCHO} + \text{R}_2\text{R}_1\text{N}-\text{CH}=\text{CH}_2 \xrightarrow[\text{HE, THF, RT}]{\text{Co, Ti, PC}}$		$\text{R}-\text{CH}(\text{OH})-\text{CH}(\text{NR}_1\text{R}_2)-\text{CH}=\text{CH}_2$			
1	2	3, 4, 5			
Aliphatic aldehydes					
3a (X=H), 91% (d.r.>20:1) 3b (X=p-Br), 82% (d.r.>20:1) 3c (X=p-OH), 78% (d.r.>20:1) 3d (X=m-CF ₃), 62% (d.r.>20:1)		3e 72% (d.r.>20:1)	3f 50% (d.r.>20:1)	3g 66% (d.r.>20:1)	
3h 65% (d.r.>20:1)	3i 40% (d.r.>20:1)	3j 80% (d.r.>20:1)	3k 60% (d.r.>20:1)	3l 47% (d.r.>20:1)	
3m 75% (d.r.>20:1)	3n 80% (d.r.>20:1)	3o 74% (d.r.>20:1)	3p 80% (d.r.>20:1)	3q 78% (d.r.>20:1)	
Aromatic aldehydes					
4a 50% (d.r.=7:1)	4b 80% (d.r.=15:1)	4c 50% (d.r.>20:1)	4d 44% (d.r.>20:1)	4e 43% (d.r.>20:1)	
4f 55% (d.r.>20:1)	4g 73% (d.r.>20:1)	4h 46% (d.r.>20:1)	4i 46% (d.r.>20:1)	4j 50% (d.r.>20:1)	
Amino allenes					
5a 52% (d.r.>20:1)	5b 83% (d.r.>20:1)	5c 88% (d.r.>20:1)	5d 85% (d.r.>20:1)	5e 90% (d.r.>20:1)	
5f 90% (d.r.>20:1)	5g 64% (d.r.>20:1)	5h 83% (d.r.>20:1)	5i 58% (d.r.>20:1)	5j 88% (d.r.>20:1)	
5k 90% (d.r.>20:1)	5m		5l 72% (d.r.>20:1)		
$\text{5k} \xrightarrow[\text{MeOH/DCM, rt}]{\text{N}_2\text{H}_4 \cdot \text{H}_2\text{O}} \text{5m} \xleftarrow[\text{EtOH:H}_2\text{O, reflux}]{\text{NH}_2\text{OH} \cdot \text{HCl}}$					
		72% yield (d.r. > 20:1)		50% yield (d.r. > 20:1)	

Reported yields are those of the isolated products. Reactions conditions: aldehydes **1** (0.5 mmol, 1 equiv), allenes **2** (2 equiv), 4CzIPN (1 mol%), Co-1 (0.1 mol%), Cp₂TiCl₂ (5 mol%), HE (2.5 equiv), collidine/HCl (0.1 equiv), THF (c=0.1 M), 10 W blue LEDs, RT, 12 h; d.r. were determined by ¹H NMR analysis of crude products.

Table 3: Scope of allylation with oxy/thio-allenes.^[a]

RCHO		+ $R_1O=C=CH_2$ or $R_2S=C=CH_2$		Co ^I Ti ^{IV} PC ^{III}	HE, THF, RT	OR ₁	SR ₂
1	6	7				8	9
	8a (X=I), 90% (d.r.= 9:1) 8b (X=OMe), 90%, (d.r.= 7:1) 8c (X=CF ₃), 88%, (d.r.= 5:1) 8d (X=CN), 92%, (d.r.= 5:1)						
	8e 74% (d.r.= 7:1)						
8h 77% (d.r.= 8:1)	8f 85% (d.r.= 10:1)	8i 80% (d.r.= 7:1)	8j 82% (d.r.= 10:1)	8k 82% (d.r.= 9:1)	8l 68% (d.r.= 8:1)	8m 87% (d.r.= 10:1)	8n 60% (d.r.= 8:1)
8o 78% (d.r.= 8:1)	8p 80% (d.r.= 9:1)	8q 66% (d.r.= 6:1)					
9a 95% (d.r.>20:1)	9b 85% (d.r.= 11:1)	9c 80% (d.r.= 12:1)	9d 94% (d.r.= 12:1)	9e 55% (d.r.= 18:1)			
9f 92% (d.r.= 13:1)	9g 75% (d.r.> 20:1)	9h 87% (d.r.= 17:1)	9i 70% (d.r.= 12:1)	9j 80% (d.r.= 16:1)			
9k 92% (d.r.= 9:1)	9l 56% (d.r.= 12:1)	9m 80% (d.r.= 9:1)	9n 74% (d.r.= 10:1)	9o 75% (E/Z =6:1) ^[b]			
9p 85% (E/Z >20:1) ^[b]	9q 83% (E/Z =8:1) ^[b]	9r 86% (E/Z =16:1) ^[b]	9s 82% (E/Z =13:1) ^[b]	9t 81% (E/Z > 20:1) ^[b]			

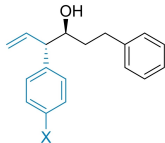
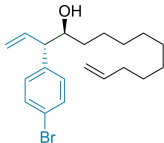
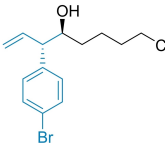
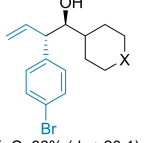
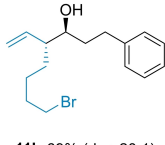
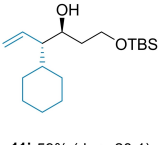
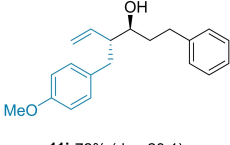
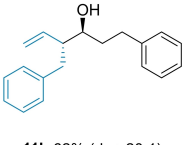
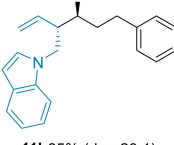
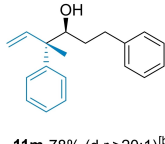
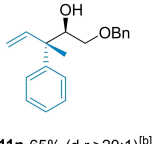
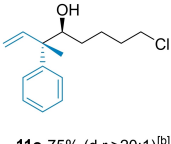
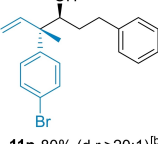
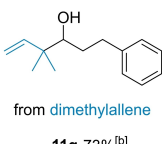
Reported yields are those of the isolated products. [a] Reactions conditions: aldehydes **1** (0.5 mmol, 1 equiv), allenes (1 mmol, 2 equiv), 4CzIPN (1 mol%) was used for **6** and Ir[dF(CF₃)ppy]₂(dtbbpy)PF₆ (1 mol%) was used for **7**, Co-**1** (0.1 mol%), Cp₂TiCl₂ (5 mol%), HE (2.5 equiv), collidine/HCl (0.1 equiv), THF (c=0.1 M), 10 W blue LEDs, RT, 12 h; d.r. were determined by ¹H NMR analysis of crude products. [b] Co-**1** (0.5 mol%) was used.

Additionally, when D₂O (4 equiv, relative to **1a**) was added as the D⁺ source into the THF solution at the beginning of the reaction, deuterium was present in the products. This result supports the generation of Co^{III}-H species through reduction of H⁺ by Co^I.

DFT calculations were performed using 1,2-allene **18** as a model to evaluate the MHAT process between the cobalt-

porphine hydride complex derived from Co-**1** and allenes (Figure 5a). The presence of collidine/HCl and Co^I species can facilitate the Co-H formation with an exothermal free energy of −14.6 kcal mol^{−1} (Figure 5c).^[52] The starting complexes (allene and Co-H) and the MHAT product **21** were singlets; however, the MHAT process might involve radical species. Therefore, an open-shell singlet method was

Table 4: Scope of allylation with various carbon-allenes.^[a]

$\text{RCHO} \quad \text{1} + \text{Alkyl-CH=C=CH}_2 \text{ or } \text{Ar-CH=C=CH}_2 \text{ or } \text{Ar-CH=C=CH}_2 \quad \text{10} \xrightarrow[\text{HE, THF, RT}]{\text{Co, Ti, PC, LED}}$		$\text{Alkyl-CH(OH)-CH=CH}_2 \text{ or } \text{Ar-CH(OH)-CH=CH}_2 \text{ or } \text{Ar-CH(OH)-CH=CH}_2 \quad \text{11}$	
 11a X=Br, 94% (d.r.>20:1) 11b X=F, 90% (d.r.>20:1) 11c X=OMe, 91% (d.r.>20:1)	 11d 63% (d.r.>20:1)	 11e 77% (d.r.>20:1)	 11f X=C, 66% (d.r.>20:1) 11g X=NBoc, 58% (d.r.>20:1)
 11h 69% (d.r.>20:1)	 11i 59% (d.r.>20:1)	 11j 72% (d.r.>20:1)	 11k 62% (d.r.>20:1)
 11l 65% (d.r.>20:1)	 11m 78% (d.r.>20:1) ^[b]	 11n 65% (d.r.>20:1) ^[b]	 11o 75% (d.r.>20:1) ^[b]
 11p 80% (d.r.>20:1) ^[b]	 11q 73% ^[b]	from dimethylallene	

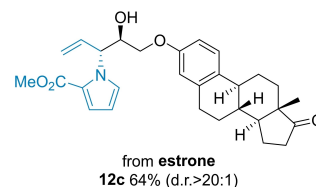
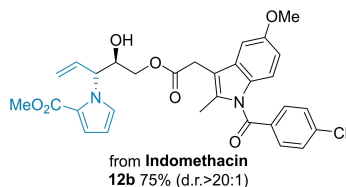
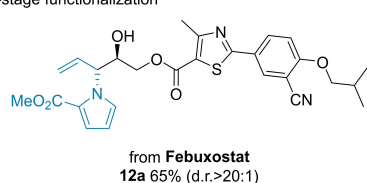
Reported yields are those of the isolated products. [a] Reactions conditions: aldehydes **1** (0.5 mmol, 1 equiv), allenes **10** (2 equiv), 4CzIPN (1 mol%), **Co-1** (0.1 mol%), Cp_2TiCl_2 (5 mol%), HE (2.5 equiv), collidine/HCl (0.1 equiv), THF ($c=0.1$ M), 10 W blue LEDs, RT, 12 h; d.r. were determined by ^1H NMR analysis of crude products. [b] **Co-1** (0.02 mol%), allenes **10** (2.5 equiv), $\text{Ir}[\text{dF}(\text{CF}_3)\text{ppy}]_2(\text{dtbbpy})\text{PF}_6$ (1 mol%) was used instead of 4CzIPN.

employed. The geometry optimizations and frequency analysis were performed in the gas phase with ωB97XD method. The Co atom was represented by the LANL2TZ(f) basis set. All atoms of the allene and 2,4,6-collidine, N atoms of the porphyrin ring, and the hydride atom were described by 6-31G(d,p) basis set. Atoms of the substituents on the porphyrin ring were described by STO-3G basis set. Other atoms of the porphyrin were described by 6-31G basis set. IRC was performed at the same level to check the transition state of MHAT process. Single point energy of the species in THF was calculated with ωB97XD method using SMD model, and all atoms were described by def2-TZVP basis set. The transition state, **TS19**, was spin-polarized (the allene moiety had excess β electron density, while the Co–H moiety had excess α electron density), exhibiting partially radical pair character (Figure 5b). Additionally, the computed Co–H (1.500 Å) and C–H (1.549 Å) bond lengths of the transition state **TS19** are elongated. After the MHAT process, an allyl radical **20a** ($S=1/2$, $m_s=-1/2$) and Co^{II} species **20b** ($S=1/2$, $m_s=1/2$) were generated. The spin-polarized state remained until recombination of the radical pair **20a** and **20b** to produce the singlet allyl– Co^{II} species **21**. DFT calculations revealed that the overall MHAT reaction was exergonic by $27.7 \text{ kcal mol}^{-1}$. The MHAT from Co–H to allene producing allyl radicals **20a** and Co^{II} species **20b** has a relatively small activation energy barrier of $13.0 \text{ kcal mol}^{-1}$ at 25°C , which complies with the experimentally observed fast reaction rate under the current conditions. Additionally, the energy barrier of homolysis of

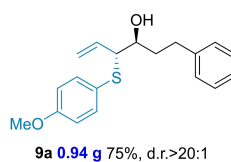
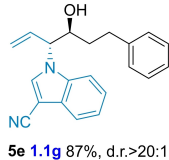
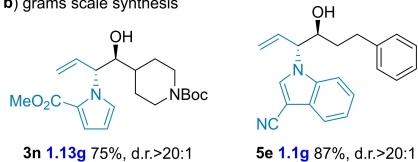
allylCobalt^{III} **21** is only $1.6 \text{ kcal mol}^{-1-1}$ indicating that it is highly unstable and readily homolyze to afford allyl radical **20a** and Co^{II} **20b** (Figure 5c).^[60–63]

Several factors contribute to the success of the reaction. Firstly, $\text{Co}(\text{Por})(\text{H})$ species lacks cis-vacant sites to the hydride, unlike other Co complexes such as **Co-5** and **Co-6**. As a result, the common migratory insertion pathway is not available. Secondly, the computed $\text{Co}(\text{por})\text{–H}$ bond dissociation enthalpies (BDE) are approximately 51 kcal mol^{-1} , which is generally considered thermodynamically stable with respect to H_2 formation, and slow for MHAT with simple alkene.^[10,11] However, quick MHAT may occur if radicals formed are stabilized. This scenario explains why the reaction system selectively functionalizes allenes without further reacting with alkenes.

Stern–Volmer analysis was conducted by fluorimetry and time-correlated single-photon counting (TCSPC) to examine the primary stage of the reaction, i.e., which molecular component quenched the excited state of 4CzIPN. Fluorimetry revealed that HE, Cp_2TiCl_2 , and **Co-1** could quench the fluorescence of 4CzIPN (Figure 6). The Stern–Volmer plot was found to deviate from linearity since 4CzIPN possesses both prompt fluorescence (PF) and thermally activated delayed fluorescence (TADF).^[64–66] Therefore, it is necessary from TCSPC data to determine their individual quenching rate constants in the two decay pathways. The results show that all three molecular components do quench both PF and TADF. In the reaction system, the concentration of HE is 50 times that of Cp_2TiCl_2

a) late-stage functionalization^a

b) grams scale synthesis



c) synthetic transformations

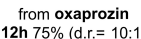
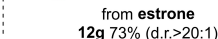
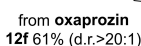
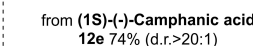
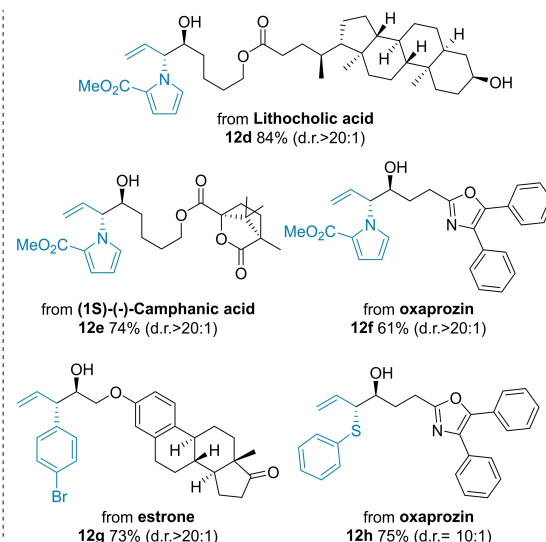
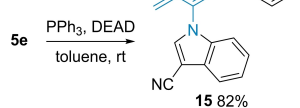
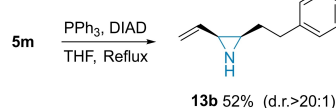
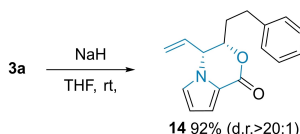
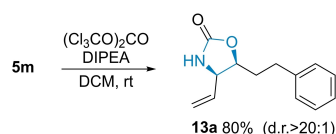


Figure 2. Synthetic applications. DIAD: diisopropyl azodicarboxylate; DEAD: diethyl azodicarboxylate; PPh₃: triphenylphosphine. a) Reactions conditions: aldehydes (0.2 mmol, 1 equiv), allenenes (2 equiv), 4CzIPN (1 mol %) [Ir[dF(CF₃)ppy]₂(dtbbpy)PF₆ (1 mol %) was used for **12h**), **Co-1** (0.1 mol %), Cp₂TiCl₂ (5 mol %), HE (2.5 equiv), collidine/HCl (0.1 equiv), THF (*c*=0.1 M), 10 W blue LEDs, RT, 12 h; d.r. were determined by ¹H NMR analysis of crude products.

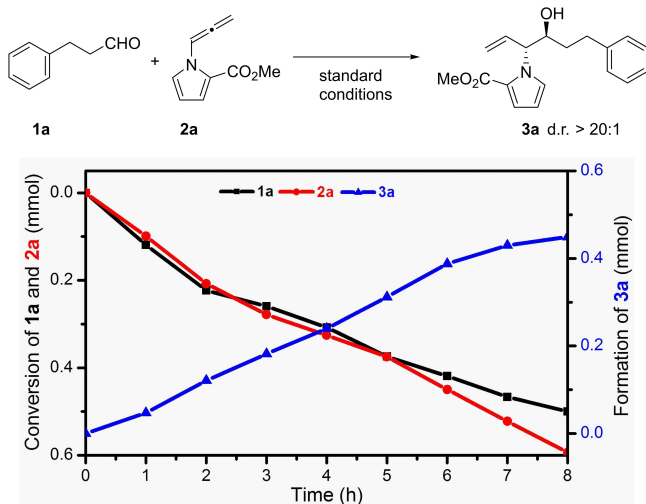


Figure 3. Reaction profile: the conversion of **1a** (black line) and **2a** (red line) corresponding the formation of **3a** (blue line). Standard conditions: **1a** (0.5 mmol, 1 equiv), **2a** (2 equiv), 4CzIPN (1 mol %), **Co-1** (0.1 mol %), Cp₂TiCl₂ (5 mol %), HE (2.5 equiv), collidine/HCl (0.1 equiv), THF (*c*=0.1 M), 10 W blue LEDs, RT, 12 h.

and 2500 times that of **Co-1**. Therefore, more than 96 % of the initial singlet excited state was quenched by HE (for details please see Supporting Information S9).

Based on the above results, we proposed the following catalytic cycle (Figure 7). First, HE ($E_{\text{HE}^{\bullet+}/\text{HE}} = +1.0 \text{ V vs SCE}$)^[67] was oxidized by the photoexcited 4CzIPN* [$E_{1/2}(4\text{CzIPN}^*/4\text{CzIPN}^{\bullet-}) = +1.43 \text{ V vs SCE}$]^[70] to produce 4CzIPN^{•+} species and HE^{•+}, which could further participate in electron transfer events and ultimately produced pyH⁺. Both Co^{II} [$E_{1/2}(\text{Co}^{\text{II}}/\text{Co}^{\text{I}}) = -0.70 \text{ V vs SCE}$]^[68] and Ti^{IV} [$E_{1/2}(\text{Ti}^{\text{IV}}/\text{Ti}^{\text{III}}) = -0.57 \text{ V vs SCE}$]^[69] species were reduced under reductive conditions by the strong reductant 4CzIPN^{•+} [$E_{1/2}(4\text{CzIPN}/4\text{CzIPN}^{\bullet-}) = -1.24 \text{ V vs SCE}$]^[70]. Then Co^I was oxidized by H⁺ to produce the Co^{III}-H^[52] species which could transfer an H atom to allene **22** generating Co^{II} and allyl radical **23**. Radical **23** was rapidly trapped by Ti^{III} to form nucleophilic π -allyltitanium complexes **24** which subsequently coupled with aldehydes. After hydrolysis by pyH⁺, the homoallylic alcohols were obtained and free Ti^{IV} was released. Finally, SET reduction of Co^I and Ti^{IV} to regenerate Co^{II} and Ti^{III}. In addition, the generating π -allylCobalt^{III} species **26** is possible according to the DFT calculations. π -allylCobalt^{III} **26** is unstable and could undergo a fast equilibrium with allyl radical **23** and Co^{II} (path I). It also could be reduced to π -allylCobalt^{II} **27** and then afforded radical **23** and Co^I (path II).^[71–73] In both cases, the catalytic cycle could be closed.

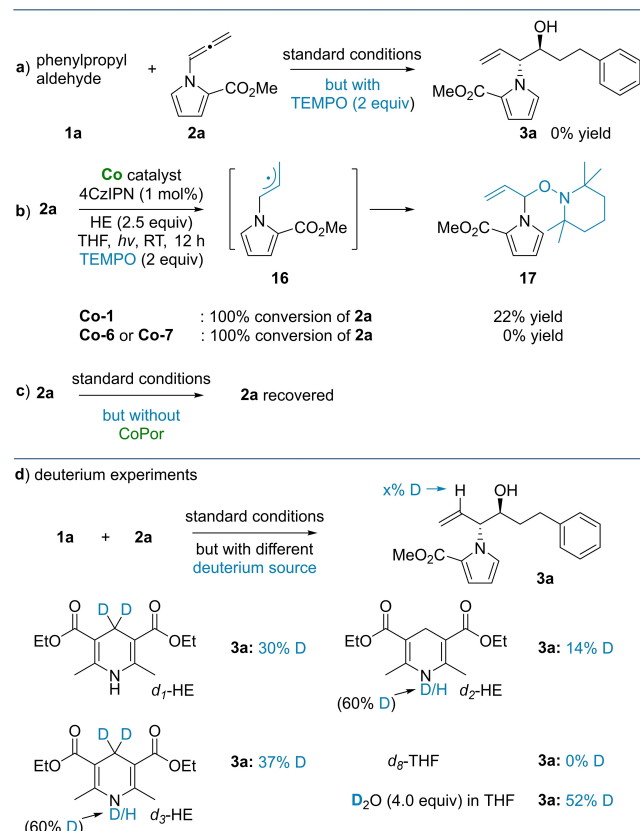


Figure 4. a)–c) Evidence of allyl radicals and the roles of Co catalysts. d) Deuterium experiments. Standard conditions: **1a** (0.5 mmol, 1 equiv), **2a** (2 equiv), 4CzIPN (1 mol%), **Co-1** (0.1 mol%), Cp_2TiCl_2 (5 mol%), HE (2.5 equiv), collidine/HCl (0.1 equiv), THF ($c=0.1$ M), 10 W blue LEDs, RT, 12 h.

Conclusion

This work reports on the photo Co-MHAT reaction for allene functionalization using Co-porphines as catalysts which exhibits exceptional activity by fine-tuning their electronic properties. Additionally, by the combination of MHAT and π -allylmetals chemistry, we developed novel bimetallic Co and Ti photoredox catalysis enabling the successful carbonyl allylation to produce vinyl-substituted 1,2-aminoalcohols, 1,2-diols and 1,2-thioalcohols with exceptional regio- and diastereoselectivity. The new metallaphotoredox strategy significantly increased the synthetic potentials of MHAT reaction and expanded the scope of the carbonyl allylation.

Acknowledgements

We appreciate the reviewers for their valuable input in enhancing the manuscript's scientific quality. Project was supported by the National Natural Science Foundation of China (22171036), Open Research Fund of School of Chemistry and Chemical Engineering, Henan Normal University (2020YB03). We thank WATTCAS CHEM-TECH

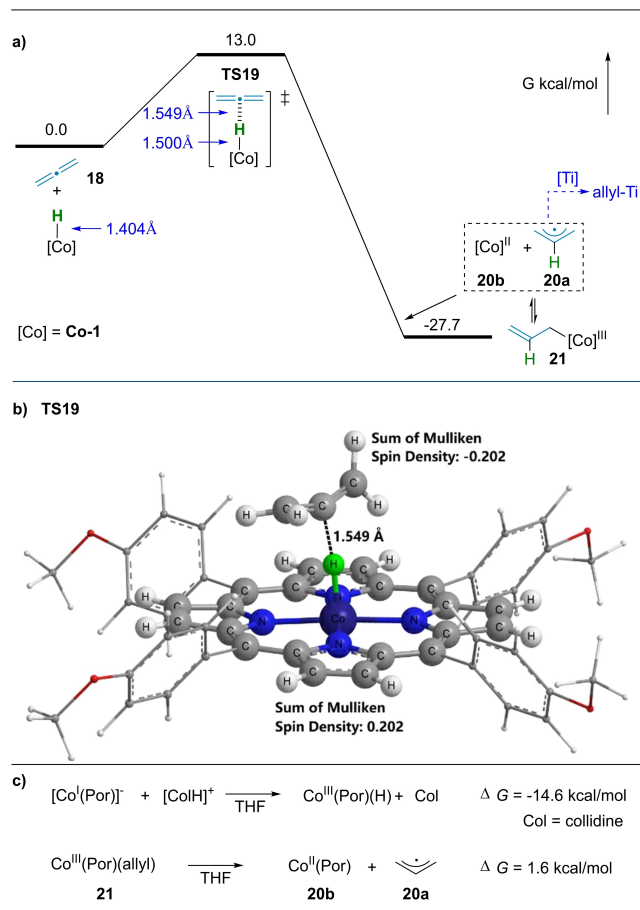


Figure 5. a) Computed energy profile of the MHAT between H-Co-1 and 1,2-allene. b) Computed structure of the transition state **TS19** of the MHAT between **Co-1** hydride complex and 1,2-allene. c) Computed thermodynamic parameters. (for details please see ESI S12).

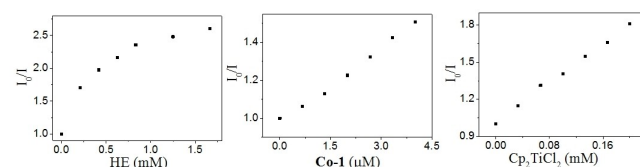


Figure 6. Stern–Volmer luminescence quenching analysis using 4CzIPN with quenchers HE (left), **Co-1** (middle) and Cp_2TiCl_2 (right).

Co., Ltd. for kindly providing the photoreactor. We acknowledge Hefei Advanced Computing Center for computational resources.

Conflict of Interest

The authors declare no conflict of interest.

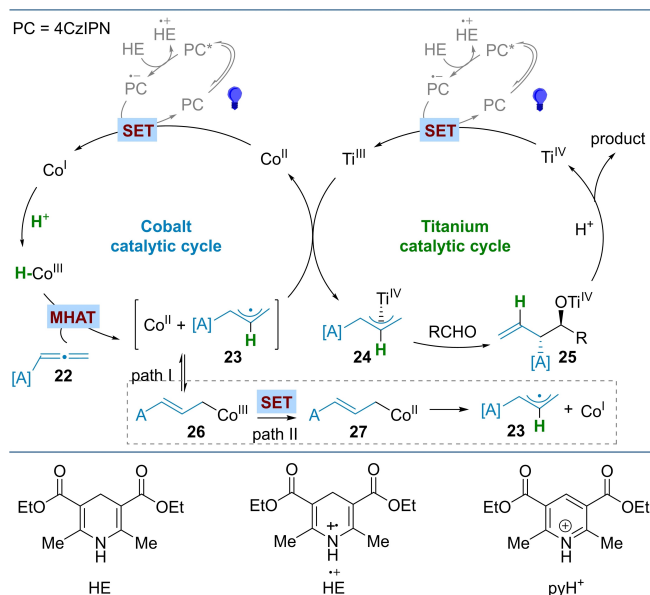


Figure 7. Proposed catalytic mechanism.

Data Availability Statement

The data that support the findings of this study are available in the Supporting Information of this article.

Keywords: Allylic Compounds • Cobalt • Photoredox Catalysis • Radicals • Reaction Mechanism

- [1] B. M. Trost, *Science* **1991**, 254, 1471–1477.
- [2] B. M. Trost, *Science* **1983**, 219, 245–250.
- [3] J. A. K. Harmony, *Methods in Free Radical Chemistry* **1974**, 5, 101–176.
- [4] L. Sandhiya, H. Jangra, H. Zipse, *Angew. Chem. Int. Ed.* **2020**, 59, 6318–6329.
- [5] J. M. Mayer, *Acc. Chem. Res.* **2011**, 44, 36–46.
- [6] J. Hartung, J. Norton, *Catalysis Without Precious Metals* (Ed.: R. M. Bullock), Wiley-VCH, Weinheim, **2010**.
- [7] T. Mukaiyama, S. Isayama, S. Inoki, K. Kato, T. Yamada, T. Takai, *Chem. Lett.* **1989**, 18, 449–452.
- [8] H. M. Feder, J. Halpern, *J. Am. Chem. Soc.* **1975**, 97, 7186–7188.
- [9] S. A. Green, S. W. M. Crossley, J. L. M. Matos, S. Vásquez-Céspedes, S. L. Shevick, R. A. Shenvi, *Acc. Chem. Res.* **2018**, 51, 2628–2640.
- [10] S. W. M. Crossley, C. Obradors, R. M. Martinez, R. A. Shenvi, *Chem. Rev.* **2016**, 116, 8912–9000.
- [11] S. L. Shevick, C. V. Wilson, S. Kotesova, D. Kim, P. L. Holland, R. A. Shenvi, *Chem. Sci.* **2020**, 11, 12401–12422.
- [12] J. Waser, B. Gaspar, H. Nambu, E. M. Carreira, *J. Am. Chem. Soc.* **2006**, 128, 11693–11712.
- [13] T. J. Barker, D. L. Boger, *J. Am. Chem. Soc.* **2012**, 134, 13588–13591.
- [14] J. C. Lo, J. Gui, Y. Yabe, C. Pan, P. S. Baran, *Nature* **2014**, 516, 343–348.
- [15] X. Ma, S. B. Herzon, *J. Am. Chem. Soc.* **2016**, 138, 8718–8721.
- [16] T. Qin, G. Lv, Q. Meng, G. Zhang, T. Xiong, Q. Zhang, *Angew. Chem. Int. Ed.* **2021**, 60, 25949–25957.

- [17] S. M. Thullen, T. Rovis, *J. Am. Chem. Soc.* **2017**, 139, 15504–15508.
- [18] G. Li, J. L. Kuo, A. Han, J. M. Abuyuan, L. C. Young, J. R. Norton, J. H. Palmer, *J. Am. Chem. Soc.* **2016**, 138, 7698–7704.
- [19] Q. Meng, T. E. Schirmer, K. Katou, B. König, *Angew. Chem. Int. Ed.* **2019**, 58, 5723–5728.
- [20] Y. Li, S. Zhang, J. Chen, J. Xia, *J. Am. Chem. Soc.* **2021**, 143, 7306–7313.
- [21] H. Cao, H. Jiang, H. Feng, J. M. C. Kwan, X. Liu, J. Wu, *J. Am. Chem. Soc.* **2018**, 140, 16360–16367.
- [22] a) Y. Kamei, Y. Seino, Y. Yamaguchi, T. Yoshino, S. Maeda, M. Kojima, S. Matsunaga, *Nat. Commun.* **2021**, 12, 966; b) M. Nakagawa, Y. Matsuki, K. Nagao, H. Ohmiya, *J. Am. Chem. Soc.* **2022**, 144, 7953–7959; c) E. Bergamaschi, V. J. Mayrhofer, C. J. Teskey, *ACS Catal.* **2022**, 12, 14806–14811; d) X. Tao, Q. Wang, L. Kong, S. Ni, Y. Pan, Y. Wang, *ACS Catal.* **2022**, 12, 15241–15248; e) X. Fang, N. Zhang, S.-C. Chen, T. Luo, *J. Am. Chem. Soc.* **2022**, 144, 2292–2300; f) A. Suzuki, Y. Kamei, M. Yamashita, Y. Seino, Y. Yamaguchi, T. Yoshino, M. Kojima, S. Matsunaga, *Angew. Chem. Int. Ed.* **2023**, 62, e202214433.
- [23] S. H. Kyne, G. Lefèvre, C. Ollivier, M. Petit, V. Ramis Cladera, L. Fensterbank, *Chem. Soc. Rev.* **2020**, 49, 8501–8542.
- [24] J. F. Garst, T. M. Bockman, R. Batlaw, *J. Am. Chem. Soc.* **1986**, 108, 1689–1691.
- [25] M. Yus, J. C. González-Gómez, F. Foubelo, *Chem. Rev.* **2013**, 113, 5595–5698.
- [26] M. Yus, J. C. González-Gómez, F. Foubelo, *Chem. Rev.* **2011**, 111, 7774–7854.
- [27] S. E. Denmark, J. Fu, *Chem. Rev.* **2003**, 103, 2763–2794.
- [28] P. Wang, M. Shen, L. Gong, *Synthesis* **2018**, 50, 956–967.
- [29] M. Holmes, L. A. Schwartz, M. J. Krische, *Chem. Rev.* **2018**, 118, 6026–6052.
- [30] K. C. Nicolaou, D. Rhoades, M. Lamani, M. R. Pattanayak, S. M. Kumar, *J. Am. Chem. Soc.* **2016**, 138, 7532–7535.
- [31] T. Biftu, R. Sinha-Roy, P. Chen, X. Qian, D. Feng, J. T. Kuethe, G. Scapin, Y. D. Gao, Y. Yan, D. Krueger, A. Bak, G. Eiermann, J. He, J. Cox, J. Hicks, K. Lyons, H. He, G. Salituro, S. Tong, S. Patel, G. Doss, A. Petrov, J. Wu, S. S. Xu, C. Sewall, X. Zhang, B. Zhang, N. A. Thornberry, A. E. Weber, *J. Med. Chem.* **2014**, 57, 3205–3212.
- [32] X. Yue, Y. Li, M. Liu, D. Sang, Z. Huang, F. Chen, *Chem. Commun.* **2022**, 58, 9010–9013.
- [33] a) R. M. Kanada, D. Itoh, M. Nagai, J. Nijima, N. Asai, Y. Mizui, S. Abe, Y. Kotake, *Angew. Chem. Int. Ed.* **2007**, 46, 4350–4355; b) T.-C. Wang, P.-S. Wang, D.-F. Chen, L. Z. Gong, *Sci. China Chem.* **2022**, 65, 298–303.
- [34] M. Lombardo, C. Trombini, *Chem. Rev.* **2007**, 107, 3843–3879.
- [35] K. Spielmann, M. Xiang, L. A. Schwartz, M. J. Krische, *J. Am. Chem. Soc.* **2019**, 141, 14136–14141.
- [36] E. Skucas, J. R. Zbieg, M. J. Krische, *J. Am. Chem. Soc.* **2009**, 131, 5054–5055.
- [37] M. Xiang, D. E. Pfaffinger, E. Ortiz, G. A. Brito, M. J. Krische, *J. Am. Chem. Soc.* **2021**, 143, 8849–8854.
- [38] Z. Wu, W. Zhang, *Chin. J. Org. Chem.* **2017**, 37, 2250–2262.
- [39] P. Knochel, W. Dohle, N. Gommermann, F. F. Kneisel, F. Kopp, T. Korn, I. Sapountzis, V. A. Vu, *Angew. Chem. Int. Ed.* **2003**, 42, 4302–4320.
- [40] H. M. Huang, P. Bellotti, F. Glorius, *Chem. Soc. Rev.* **2020**, 49, 6186–6197.
- [41] H. Huang, M. Koy, E. Serrano, P. M. Pflüger, J. L. Schwarz, F. Glorius, *Nat. Catal.* **2020**, 3, 393–400.
- [42] H. Huang, P. Bellotti, P. M. Pflüger, J. L. Schwarz, B. Heidrich, F. Glorius, *J. Am. Chem. Soc.* **2020**, 142, 10173–10183.
- [43] J. L. Schwarz, F. Schäfers, A. Tlahuext-Aca, L. Lückemeier, F. Glorius, *J. Am. Chem. Soc.* **2018**, 140, 12705–12709.
- [44] Y. Xiong, G. Zhang, *J. Am. Chem. Soc.* **2018**, 140, 2735–2738.

- [45] a) S. Tanabe, H. Mitsunuma, M. Kanai, *J. Am. Chem. Soc.* **2020**, *142*, 12374–12381; b) P.-Z. Wang, X. Wu, Y. Cheng, M. Jiang, W.-J. Xiao, J.-R. Chen, *Angew. Chem. Int. Ed.* **2021**, *60*, 22956–22962; c) J. Chen, Y.-J. Liang, P.-Z. Wang, G.-Q. Li, B. Zhang, H. Qian, X.-D. Huan, W. Guan, W.-J. Xiao, J.-R. Chen, *J. Am. Chem. Soc.* **2021**, *143*, 13382–13392.
- [46] A. Y. Chan, I. B. Perry, N. B. Bissonnette, B. F. Buksh, G. A. Edwards, L. I. Frye, O. L. Garry, M. N. Lavagnino, B. X. Li, Y. Liang, E. Mao, A. Millet, J. V. Oakley, N. L. Reed, H. A. Sakai, C. P. Seath, D. W. C. MacMillan, *Chem. Rev.* **2022**, *122*, 1485–1542.
- [47] J. Twilton, C. Le, P. Zhang, M. H. Shaw, R. W. Evans, D. W. C. MacMillan, *Nat. Chem. Rev.* **2017**, *1*, 52.
- [48] K. L. Skubi, T. R. Blum, T. P. Yoon, *Chem. Rev.* **2016**, *116*, 10035–10074.
- [49] a) M. Kojima, S. Matsunaga, *Trends Chem.* **2020**, *2*, 410–426; b) D. Zhang, H. Li, Z. Guo, Y. Chen, H. Yan, Z. Ye, F. Zhang, B. Lu, E. Hao, L. Shi, *Green Chem.* **2022**, *24*, 9027–9032; c) C. Shi, F. Li, Y. Chen, S. Lin, E. Hao, Z. Guo, U. T. Wosqa, D. Zhang, L. Shi, *ACS Catal.* **2021**, *11*, 2992–2998; d) X. Jiang, H. Jiang, Q. Yang, Y. Cheng, L.-Q. Lu, J. A. Tunge, W.-J. Xiao, *J. Am. Chem. Soc.* **2022**, *144*, 8347–8354.
- [50] a) Z. Zhang, T. Hilche, D. Slak, N. R. Rietdijk, U. N. Oloyede, R. A. Flowers, A. Gansäuer, *Angew. Chem. Int. Ed.* **2020**, *59*, 9355–9359; b) Z. Zhang, R. B. Richrath, A. Gansäuer, *ACS Catal.* **2019**, *9*, 3208–3212; c) F. Calogero, G. Magagnano, S. Potenti, F. Pasca, A. Fermi, A. Gualandi, P. Ceroni, G. Bergamini, P. G. Cozzi, *Chem. Sci.* **2022**, *13*, 5973–5981; d) A. Gualandi, F. Calogero, M. Mazzarini, S. Guazzi, A. Fermi, G. Bergamini, P. G. Cozzi, *ACS Catal.* **2020**, *10*, 3857–3863; e) F. Calogero, A. Gualandi, M. D. Matteo, S. Potenti, A. Fermi, G. Bergamini, P. G. Cozzi, *J. Org. Chem.* **2021**, *86*, 7002–7009; f) F. Li, S. Lin, Y. Chen, C. Shi, H. Yan, C. Li, C. Wu, L. Lin, C. Duan, L. Shi, *Angew. Chem. Int. Ed.* **2021**, *60*, 1561–1566; g) F. Li, Y. Chen, S. Lin, C. Shi, X. Li, Y. Sun, Z. Guo, L. Shi, *Org. Chem. Front.* **2020**, *7*, 3434–3438; h) S. Lin, Y. Chen, F. Li, C. Shi, L. Shi, *Chem. Sci.* **2020**, *11*, 839–844; i) M. Yamane, Y. Kanzaki, H. Mitsunuma, M. Kanai, *Org. Lett.* **2022**, *24*, 1486–1490.
- [51] a) A. Fermi, A. Gualandi, G. Bergamini, P. G. Cozzi, *Eur. J. Org. Chem.* **2020**, 6955–6965; b) Y. Chen, S. Lin, F. Li, X. Zhang, L. Lin, L. Shi, *ChemPhotoChem* **2020**, *4*, 659–663.
- [52] X. Li, B. Lv, X. P. Zhang, X. Jin, K. Guo, D. Zhou, H. Bian, W. Zhang, U. P. Apfel, R. Cao, *Angew. Chem. Int. Ed.* **2022**, *61*, e202114310.
- [53] A. Call, C. Casadevall, F. Acuña-Parés, A. Casitas, J. Lloret-Fillol, *Chem. Sci.* **2017**, *8*, 4739–4749.
- [54] F. Schäfers, L. Quach, J. L. Schwarz, M. Saladrigas, C. G. Daniliuc, F. Glorius, *ACS Catal.* **2020**, *10*, 11841–11847.
- [55] a) T. Michiyuki, K. Komeyama, *Asian J. Org. Chem.* **2019**, *9*, 343–358; b) T. Okamoto, S. Oka, *J. Org. Chem.* **1984**, *49*, 1589–1594; c) K. Sugamoto, *Synlett* **1998**, *1998*, 1270–1272; d) K. Sugamoto, Y. Matsushita, T. Matsui, *J. Chem. Soc. Perkin Trans. 1* **1998**, 3989–3998.
- [56] L. Pitzer, F. Schäfers, F. Glorius, *Angew. Chem. Int. Ed.* **2019**, *58*, 8572–8576.
- [57] H. Xie, B. Breit, *ACS Catal.* **2022**, *12*, 3249–3255.
- [58] M. Xiang, A. Ghosh, M. J. Krische, *J. Am. Chem. Soc.* **2021**, *143*, 2838–2845.
- [59] E. Y. Tsai, R. Y. Liu, Y. Yang, S. L. Buchwald, *J. Am. Chem. Soc.* **2018**, *140*, 2007–2011.
- [60] Y. Abderrazak, A. Bhattacharyya, O. Reiser, *Angew. Chem. Int. Ed.* **2021**, *60*, 21100–21115.
- [61] W. Mikolajski, G. Baum, W. Massa, R. W. Hoffmann, *J. Organomet. Chem.* **1989**, *376*, 397–405.
- [62] B. de Bruin, W. I. Dzik, S. Li, B. B. Wayland, *Chem. Eur. J.* **2009**, *15*, 4312–4320.
- [63] M. Ociepa, A. J. Wierzb, J. Turkowska, D. Gryko, *J. Am. Chem. Soc.* **2020**, *142*, 5355–5361.
- [64] B. Limburg, À. Cristòfol, A. W. Kleij, *J. Am. Chem. Soc.* **2022**, *144*, 10912–10920.
- [65] À. Cristòfol, B. Limburg, A. W. Kleij, *Angew. Chem. Int. Ed.* **2021**, *60*, 15266–15270.
- [66] M. A. Bryden, E. Zysman-Colman, *Chem. Soc. Rev.* **2021**, *50*, 7587–7680.
- [67] P. Z. Wang, J. R. Chen, W. J. Xiao, *Org. Biomol. Chem.* **2019**, *17*, 6936–6951.
- [68] M. Guergueb, S. Nasri, J. Brahmi, F. Loiseau, F. Molton, T. Roisnel, V. Guérineau, I. Turowska-Tyrk, K. Aouadi, H. Nasri, *RSC Adv.* **2020**, *10*, 6900–6918.
- [69] M. Parasram, B. J. Shields, O. Ahmad, T. Knauber, A. G. Doyle, *ACS Catal.* **2020**, *10*, 5821–5827.
- [70] E. Speckmeier, T. G. Fischer, K. Zeitler, *J. Am. Chem. Soc.* **2018**, *140*, 15353–15365.
- [71] J. L. M. Matos, S. Vázquez-Céspedes, J. Gu, T. Oguma, R. A. Shenoi, *J. Am. Chem. Soc.* **2018**, *140*, 16976–16981.
- [72] L. Wang, L. Wang, M. Li, Q. Chong, F. Meng, *J. Am. Chem. Soc.* **2021**, *143*, 12755–12765.
- [73] A. Bakac, J. H. Espenson, *J. Am. Chem. Soc.* **1984**, *106*, 5197–5202.

Manuscript received: February 17, 2023

Accepted manuscript online: April 12, 2023

Version of record online: May 4, 2023